Function of Integrin-Linked Kinase in Modulating the Stemness of IL-6–Abundant Breast Cancer Cells by Regulating γ-Secretase–Mediated Notch1 Activation in Caveolae[1,2]

En-Chi Hsu[*], Samuel K. Kulp[*], Han-Li Huang[*,3], Huang-Ju Tu[*,3], Santosh B. Salunke[*], Nicholas J. Sullivan[†], Duxin Sun[§], Max S. Wicha[¶], Charles L. Shapiro[‡,4] and Ching-Shih Chen[*,#]

[*]Division of Medicinal Chemistry and Pharmacognosy, College of Pharmacy, The Ohio State University Comprehensive Cancer Center, Columbus, OH, USA; [†]Department of Molecular Virology, Immunology, and Medical Genetics, The Ohio State University Comprehensive Cancer Center, Columbus, OH, USA; [‡]Division of Medical Oncology, Department of Internal Medicine, College of Medicine, The Ohio State University Comprehensive Cancer Center, Columbus, OH, USA; [§]Department of Pharmaceutical Sciences, College of Pharmacy, University of Michigan Comprehensive Cancer Center, Ann Arbor, MI, USA; [¶]Department of Internal Medicine, University of Michigan Comprehensive Cancer Center, Ann Arbor, MI, USA; [#]Institute of Biological Chemistry, Academia Sinica, Taipei, Taiwan

Abstract

Interleukin-6 (IL-6) and Notch signaling are important regulators of breast cancer stem cells (CSCs), which drive the malignant phenotype through self-renewal, differentiation, and development of therapeutic resistance. We investigated the role of integrin-linked kinase (ILK) in regulating IL-6–driven Notch1 activation and the ability to target breast CSCs through ILK inhibition. Ectopic expression/short hairpin RNA-mediated knockdown of ILK, pharmacological inhibition of ILK with the small molecule T315, Western blot analysis, immunofluorescence, and luciferase reporter assays were used to evaluate the regulation of IL-6–driven Notch1 activation by ILK in IL-6–producing triple-negative breast cancer cell lines (MDA-MB-231, SUM-159) and in MCF-7 and MCF-7[IL-6] cells. The effects of ILK on γ-secretase complex assembly and cellular localization were determined by immunofluorescence, Western blots of membrane fractions, and immunoprecipitation. *In vivo* effects of T315-induced ILK inhibition on CSCs in SUM-159 xenograft models were assessed by mammosphere assays, flow cytometry, and tumorigenicity assays. Results show that the genetic knockdown or pharmacological inhibition of ILK suppressed Notch1 activation and the abundance of the γ-secretase components presenilin-1, nicastrin, and presenilin enhancer 2 at the posttranscriptional level via inhibition of caveolin-1-dependent membrane assembly of the γ-secretase complex. Accordingly, knockdown of ILK inhibited breast CSC-like properties *in vitro* and the breast CSC

subpopulation *in vivo* in xenograft tumor models. Based on these findings, we propose a novel function of ILK in regulating γ-secretase–mediated Notch1 activation, which suggests the targeting of ILK as a therapeutic approach to suppress IL-6–induced breast CSCs.

Neoplasia (2015) 17, 497–508

Introduction

Cancer stem cells (CSCs) or tumor-initiating cells represent a small subpopulation of tumor cells harboring the capacity of self-renewal and multilineage differentiation, thereby providing a reservoir of cells that maintain the heterogeneous population of the tumor [1]. Moreover, preclinical and clinical data have suggested that CSCs are responsible for tumor recurrence after chemotherapy or radiation therapy as these cells can survive and repopulate the tumor with drug-resistant phenotype [2]. Thus, targeting the tumor cell subpopulation that exhibits stem cell–like properties will help improve outcomes for patients with cancer [3].

Accumulating evidence suggests an intricate relationship between interleukin-6 (IL-6) and Notch signaling in regulating breast CSCs [3]. For example, IL-6 has been reported to promote breast cancer bone metastasis through Notch1 [4] and to induce mammosphere formation in breast cancer cells through Notch3 [5]. Signaling through Notch involves four receptor isoforms (Notch1-4) and at least five ligands (Jagged1/2, Delta-like 1/3/4) in mammals. Activation of Notch through ligand binding stimulates γ-secretase, an enzyme complex consisting of the catalytic component pre-senilin-1 (PS1) and the three cofactors nicastrin (NCT), the presenilin enhancer 2 (PEN-2), and the anterior pharynx-defective protein 1, leading to the cleavage of Notch and release of the Notch intracellular domain (NICD) into the cytoplasm. Subsequently, Notch^{NICD} enters the nucleus to act as a transcriptional co-activator for the expression of Notch target genes, including those encoding hairy and enhancer of split-1 (HES1), hairy/enhancer-of-split related with YRPW motif protein 1 (HEY1), ATP-binding cassette subfamily G member 2 (ABCG2), and c-myc. The oncogenic role of this Notch activation was demonstrated by the promotion of breast tumorigenesis *in vivo* by Notch1^{NICD} or Notch3^{NICD} in transgenic animals [6,7]. Moreover, clinical samples show an association between elevated expression of Notch ligands/receptors and poor outcome in patients with breast cancer, especially those of triple negative breast cancer [8,9]. Therefore, therapeutic targeting of the Notch pathway might represent a relevant strategy for improving outcomes in breast cancer [10].

Integrin-linked kinase (ILK) is an integrin-interacting protein with serine/threonine kinase activity that phosphorylates Akt, glycogen synthase kinase 3β (GSK3β), integrin β1/β3, α chain nascent polypeptide-associated complex, myosin phosphatase targeting sub-unit 1, and myosin light chain 2 in a cell line– and/or context-specific manner [11]. Substantial evidence has demonstrated the involvement of ILK in regulating processes associated with aggressive phenotype, such as cell proliferation, survival, migration, and invasion, and its expression correlates with tumor grade and poor patient outcome in multiple cancer types [12]. The majority of ILK is localized to the membrane as a scaffold protein where it forms complexes with various partners, including pinch, parvin, paxillin, phosphoinositide-dependent

kinase 1, Akt, rictor, Src, integrin β1/β3, and F-actin. ILK is responsive to extracellular signals transduced through integrin or receptor tyrosine kinases in the membrane to regulate the actin cytoskeleton, stabilize microtubules, and transfer intracellular signaling cascades [13].

The functional link between ILK and Notch was first reported in leukemic cells, in which ILK acts as a critical prosurvival factor [14]. It was found that pharmacological inhibition of ILK by the small-molecule inhibitor QLT0267 blocked Notch activation through the suppression of Akt/GSK3β signaling. In addition, ILK was shown to activate Notch through a Wnt-dependent mechanism in the course of chicken embryo somitogenesis [15]. Conversely, ILK has been reported to suppress Notch activation in NIH3T3 mouse embryonic fibroblast and human embryonic kidney–293 cells by direct binding and phosphorylation of Notch1^{NICD}, leading to Fbw7-mediated degradation [16]. These conflicting results might arise from a cell type– and/or cellular context–specific role of ILK in regulating Notch activation, which warrants investigation.

Previously, we demonstrated that ILK is involved in regulating the IL-6–nuclear factor (NF)-κB signaling in breast cancer by acting as a downstream effector induced by IL-6 (unpublished data). In this study, we obtained evidence that ILK plays a crucial role in IL-6–driven Notch1 activation by regulating the integrity of the γ-secretase complex in caveolae, a type of lipid raft that forms distinct cup-shaped invaginations in the plasma membrane, in a caveolin-1–dependent manner. shRNA-mediated knockdown or pharmacological inhibition of ILK suppressed the expression of Notch1^{NICD} and downstream targets in IL-6–producing MDA-MB-231 and SUM-159 cells, as well as MCF-7^{IL-6} cells (an IL-6–overexpressing stable clone of MCF-7) [17]. Conversely, overexpression of ILK in MCF-7 cells upregulated Notch signaling. Our data suggest that IL-6–induced Notch activation by ILK was attributable to its ability to regulate the assembly/stability of the γ-secretase complex in caveolae. It is noteworthy that ILK inhibition, through knockdown or pharmacological inhibition, diminished the expression of PS1, NCT, and PEN-2 at the posttranscriptional level and, consequently, the membrane assembly of the γ-secretase complex. Furthermore, the ability of ILK to regulate Notch1 signaling was manifested by the suppressive effect of short hairpin (sh)RNA-mediated ILK knockdown on breast CSC-like properties *in vitro* and the breast CSC subpopulation *in vivo* in xenograft tumor models. On the basis of these findings, we propose a novel mechanism by which ILK regulates Notch activation by facilitating γ-secretase complex assembly in caveolae, which might foster new therapeutic strategies for targeting IL-6–induced breast CSC.

Materials and Methods

Detailed descriptions and additional information on agents, antibodies, cell culture, lentivirus preparation, immunoblot analysis, reporter assays, and other methods, as indicated below, are provided in the Supplementary Methods.

Transfection

Cells were transfected with various plasmids or small interfering (si)RNAs using an Amaxa Nucleofection system (Amaxa Biosystems, Gaithersburg, MD) or Lipofectamine 2000 (Life Technologies, Carlsbad, CA) according to the manufacturers' instructions. Detailed information on plasmid constructs are provided in the Supplementary Methods.

Mammosphere Formation Assays

Cancer cells (500 single cells in 1 ml medium per well) were plated onto ultralow attachment 24-well plates (Corning Inc, Union City, CA) and maintained in MammoCult Human Medium (Stemcell Technologies, Vancouver, Canada). Cells were treated with test agent or DMSO for 7 days, and the number of primary mammospheres with diameters greater than 50 μm was counted at ×40 magnification using a microscope fitted with a ruler. All experiments were performed at least in triplicate.

RNA Isolation and Real-Time Quantitative Polymerase Chain Reaction

Total RNA isolation, reverse transcription, and real-time quantitative polymerase chain reaction were performed using standard procedures, as described in the Supplementary Methods. All samples including the control without a template were assayed in triplicate. The relative number of target transcripts was normalized to the number of human 18S transcripts found in the same sample. The relative quantification of target gene expression was performed with the comparative cycle threshold (C_T) method.

Detergent Solubilization of γ-Secretase Complexes and Blue Native Polyacrylamide Gel Electrophoresis

Cell membrane fractions were solubilized under native conditions using 0.5% n-dodecyl β-D-maltoside on ice for 10 minutes. An equal amount of protein from each sample was loaded per lane and separated by electrophoresis on a 4% to 12% gradient Blue Native Gel (Jule, Inc, Milford, CT) according to a procedure described by the NativePAGE Novex Bis-Tris Gel System (Life Technologies), in which NativeMark Unstained Protein Standard (Life Technologies) was used as protein markers. After separation, proteins were treated with 0.1% sodium dodecyl sulfate (SDS), transferred to polyvinylidene fluoride membranes by using NuPAGE Transfer Buffer (Life Technologies), and probed with specific antibodies.

Lipid Raft Isolation and Dot Blot Analysis

Lipid raft proteins were isolated using the FOCUS Signal Protein Isolation kit (G Biosciences, St Louis, MO) according to the manufacturer's instruction, the details of which are provided in the Supplementary Methods. To determine lipid raft isolation efficiency, 1 μl of serially diluted cell lysate from fractions with equivalent protein content were dot-blotted on nitrocellulose membrane (GE Healthcare Amersham). After drying, the membrane strip was blocked with 5% milk in TBS buffer and then incubated with HRP-conjugated cholera toxin (200 ng/ml; Life Technologies) in Tris-buffered saline with Tween-20 (TBST) buffer to detect the lipid raft marker, ganglioside GM1, which was visualized by chemiluminescence (Supplementary Figure S1).

Immunofluorescence Analysis

Immunofluorescence was performed on cells seeded onto round cover glasses in 24-well culture plates. To assess γ-secretase activity, MDA-MB-231 cells were transfected with GFP-C99 for 24 hours and then treated with 2 μM T315, 10 μM N-[N-(3,5-difluorophenacetyl)-L-alanyl]-S-phenylglycine t-butyl ester (DAPT), or DMSO control. Cells were then fixed with 3.7% formaldehyde in phosphate-buffered saline (PBS) buffer for 10 minutes at room temperature and then permeabilized with PBS containing 0.5% Triton X-100 for 5 minutes at room temperature. For experiments to detect endogenous Notch1[NICD] or to examine localization of endogenous caveolin-1, γ-secretase, and lipid raft, after treatments, cells were fixed, permeabilized, blocked in 1% BSA in PBS buffer, and then incubated with primary antibodies (1:200 dilution) to Notch1V[1754], PS1, and caveolin-1 followed by Alexa Fluor 488– or Alexa Fluor 555–conjugated secondary antibodies (1:200 dilution), each for 2 hours in PBS at room temperature. Lipid rafts were labeled by incubating with Alexa Fluor 647–conjugated cholera toxin (100 ng/ml) (Life Technologies) at the same time as secondary antibody incubation. Nuclear staining and image acquisition are described in the Supplementary Methods.

Caveolin-1 Co-Immunoprecipitation

Immunoprecipitation of caveolin-1 was conducted by following a published procedure with slight modifications [18]. n-Octyl D-glucopyranoside (OCTG) was used as the sole detergent in light of its ability to solubilize caveolin-1 and caveolin-1–associated proteins [19]. Briefly, cells were lysed in iced OCTG buffer (50 mM Tris, pH 7.5, 150 mM NaCl, 0.05% SDS, 0.5% Triton X-100, and 60 mM OCTG), supplemented with protease inhibitor cocktail (Sigma) and phosphatase inhibitors (10 mM NaF, 2 mM NaVO₄, and 60 mM β-glycerophosphate), for 45 minutes, and centrifuged at 12,000 rpm at 4°C for 10 minutes. Aliquots containing equal amounts of total protein were incubated with anti–caveolin-1 or rabbit IgG negative control antibodies at 4°C for 2 hours, followed by protein A/G sepharose beads (Santa Cruz Biotechnology, Santa Cruz, CA) at 4°C for overnight. The immunoprecipitates were washed three times with OCTG buffer and resuspended in SDS sample buffer. Caveolin-1–interacting proteins were examined by immunoblot analysis.

ALDEFLUOR Assays

The ALDEFLUOR kit (StemCell Technologies) was used to isolate cell populations with high aldehyde dehydrogenase enzymatic activity as described in the manufacturer's instructions, the details of which are provided in the Supplementary Methods. Using a FACSCalibur flow cytometer, ALDEFLUOR fluorescence was excited at 488 nm, and fluorescence emission was detected using a standard fluorescein isothiocyanate filter. The gating region of the ALDH[br] population was established on the basis of negative controls.

Animal Studies

Additional details covering mouse strain, husbandry, regulatory approval, and methods are provided in Supplementary Methods.

To validate the importance of ILK for tumor initiation in vivo, MDA-MB-231 cells stably expressing ILK shRNA were injected (5 × 10⁴ cells/0.1 ml) into the left inguinal mammary fat pad of female nonobese diabetic/severe combined immunodeficiency (NOD/SCID) mice. The same number of control shRNA-transfected MDA-MB-231 cells was injected into the contralateral mammary fat pad. Tumors were measured with calipers, and the volumes were calculated weekly.

The ability of ILK inhibition by T315 to target breast CSCs in vivo was evaluated in an established SUM-159 xenograft tumor model [20]. Tumors were established by injection of SUM-159 cells (2 × 10⁶ cells/0.1 ml) into the mammary fat pads of female

NOD/SCID mice. When tumors reached a volume of 50 to 70 mm^3, mice were randomized to two groups (n = 4-5) that received T315 (50 mg/kg) or vehicle twice daily by oral gavage for 11 days. At the end of drug treatment, the mice were humanely killed, and tumors were harvested and dissociated for evaluation of the CSC subpopulation by ALDEFLUOR assay and mammosphere formation as described above and by tumorigenicity after reimplantation into secondary, tumor-naive NOD/SCID mice in which the emergence of tumors was monitored twice weekly by palpation for up to 49 days post-injection.

Statistical Analysis

Statistical differences between group means for the mammosphere formation assays, reporter assays, ALDEFLOUR assays, and SUM-159 tumor growth experiments were determined using unpaired t tests. For the MDA-MB-231 tumor growth experiment, paired t tests were used. All tests were two-sided. Differences were considered significant at $P < .05$.

Results

Evidence that ILK Regulates Notch1 Activation

Pursuant to our finding that ILK is a downstream effector of IL-6 (unpublished), we examined the potential role of ILK as a mechanistic link in IL-6–induced Notch1 activation by using a stable clone of the IL-6–overexpressing MCF-7^{IL-6} cells that overexpress ILK shRNA under Tet-on control (MCF-7$^{IL-6/TRE-shILK}$). As shown, in the absence of doxycycline, MCF-7$^{IL-6/TRE-shILK}$ cells, relative to MCF-7 parental cells, exhibited substantially higher expression of ILK and

phosphorylation of Akt, accompanied by a greater Notch1 activation, as manifested by Notch1^{NICD} accumulation (Figure 1A), and increased mammosphere formation in anchorage-independent, serum-free culture conditions (Figure 1B), a surrogate measure of CSC expansion [21]. Doxycycline-induced ILK knockdown led to reduced Akt phosphorylation and Notch1^{NICD} expression (Figure 1A) and reduced mammosphere-forming ability (Figure 1B). Furthermore, ectopic expression of ILK mimicked the effect of IL-6 overexpression on Notch1 activation in MCF-7 cells (Figure 1C), suggesting the intermediary role of ILK in this IL-6–induced cellular response. It is noteworthy that these changes in Notch1^{NICD} abundance were not accompanied by parallel changes in endogenous Notch1 expression, indicating that these effects were mediated through the regulation of Notch1 cleavage. Similarly, shRNA-mediated knockdown of ILK in two IL-6–producing triple negative breast cancer cell lines, MDA-MB-231 and SUM-159, which express higher levels of ILK and Notch1^{NICD} relative to the IL-6–deficient MCF-7 and MDA-MB-468 cells (Figure 1E), also resulted in the suppression of Notch1 activation (Figure 1D), indicating that this is not a cell line–specific phenomenon.

Our data revealed that in MCF-7^{IL-6}, MDA-MB-231, and SUM-159 cells, ILK acts as a downstream effector of IL-6 to facilitate Akt phosphorylation. As Akt has been shown to activate Notch1 gene expression through NF-κB in melanoma [22], we examined the plausible link between Akt and IL-6–driven Notch1 activation, which, however, was refuted by lack of suppressive effect of the phosphoinositide 3-kinase (PI3K) inhibitor LY294002 on Notch1^{NICD} accumulation in MCF-7^{IL-6} cells (Figure 1F)
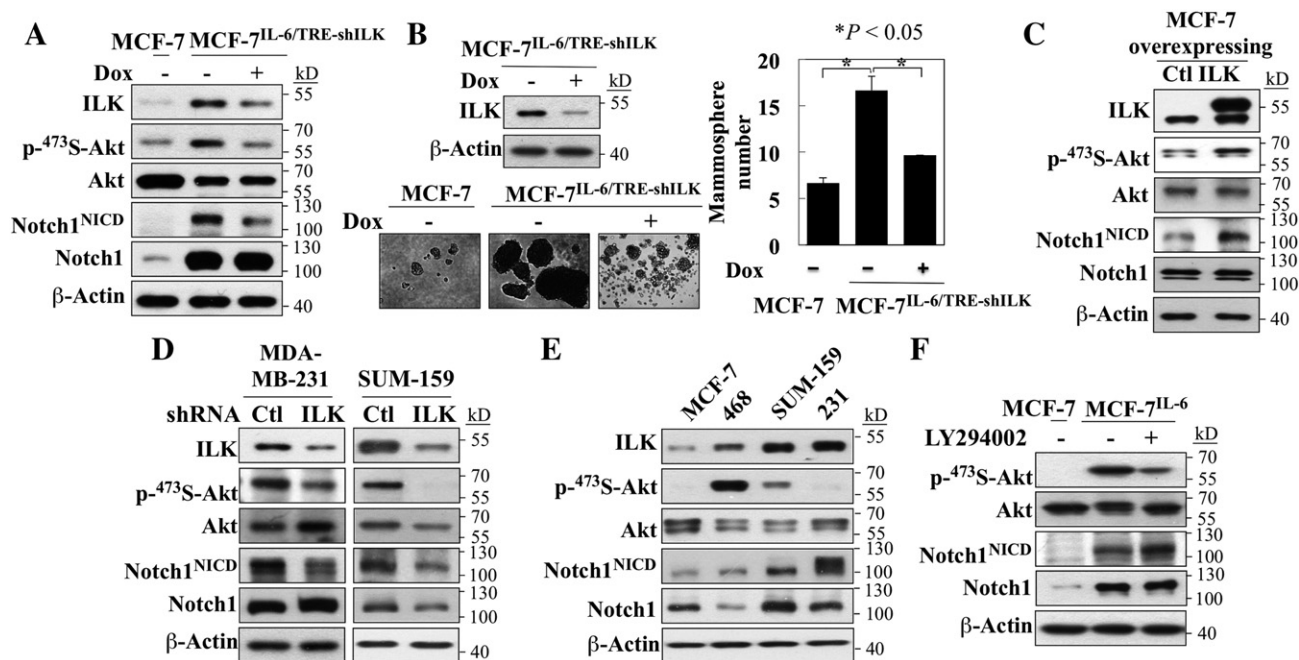

Figure 1. ILK regulated Notch activation. The effects of doxycycline (Dox)–inducible shRNA-mediated knockdown of ILK in MCF-7$^{IL-6/TRE-shILK}$ cells on (A) the expression/activation status of ILK and the IL-6 downstream signaling markers Akt and Notch1 by Western blot and (B) mammosphere formation. Data are presented as means ± SD (n = 3). (C and D) Immunoblot analysis of the effects of (C) ectopic expression of ILK in MCF-7 cells and (D) shRNA-mediated knockdown of ILK in MDA-MB-231 and SUM-159 cells on the expression/activation status of ILK, Akt, and Notch1. (E and F) Immunoblot analysis of (E) the differential expression/activation status of ILK, Akt, and Notch1 among four different breast cancer cell lines, and (F) the effect of the PI3K inhibitor, LY294002 (20 μM), on the expression/activation status of Notch1 and Akt in MCF-7^{IL-6} cells.
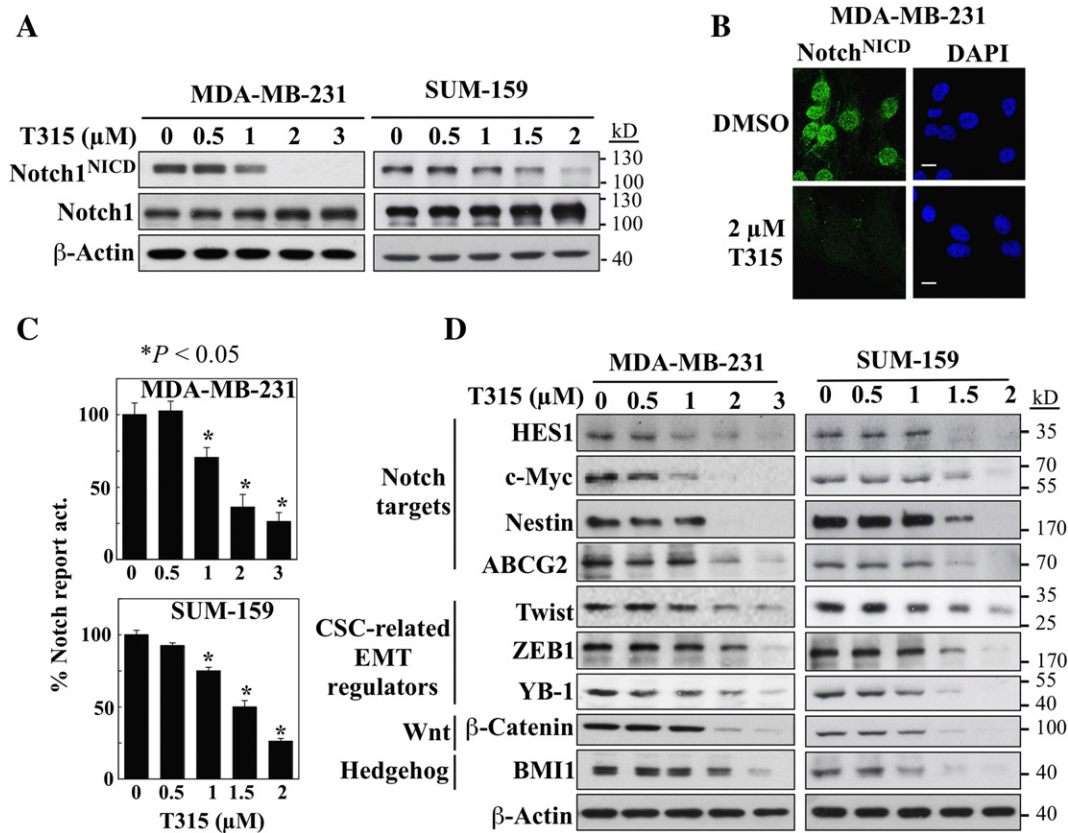
Figure 2. The ILK inhibitor, T315, suppressed Notch activation. (A) Immunoblot analysis of the dose-dependent effects of T315 on the expression/activation status of Notch1 in MDA-MB-231 and SUM-159 cells. (B) Immunocytochemical analysis of the effect of T315 *versus* DMSO control on the nuclear localization of Notch1^{NICD} (using an antibody specific for the Notch1V^{1744} cleavage epitope) in MDA-MB-231 cells (original magnification, × 40; scale bar, 10 μm). DAPI, 4′,6-diamidino-2-phenylindole. (C) Dose-dependent suppressive effects of T315 on Notch activation in MDA-MB-231 and SUM-159 cells expressing a luciferase reporter containing a Notch activation–responsive transcriptional response element. Data are presented as means ± SD (n = 3). (D) Dose-dependent suppressive effects of T315 on protein expression of biomarkers associated with CSC signaling pathways mediated by Notch (HES1, c-Myc, Nestin, ABCG2), Wnt (β-catenin), and hedgehog (Bmi1) and with epithelial-mesenchymal transition (ZEB1, Twist, and Y box-binding protein 1) in MDA-MB-231 and SUM-159 cells.

Pharmacological Inhibitor of ILK by T315 Blocks Notch1 Activation

We further interrogated the role of ILK in mediating IL-6–driven Notch1 activation by using the small-molecule inhibitor T315 as a proof-of-concept compound, which inhibited the kinase activity of immunoprecipitated ILK with inhibitory concentration 50 (IC$_{50}$) of 0.6 μM [23] and suppressed the viability of breast cancer cells with high potency (IC$_{50}$: MCF-7, 2.7 μM; MCF-7^{IL-6}, 3.5 μM; MDA-MB-231, 1.8 μM; SUM-159, 1.5 μM). Reminiscent of effects observed with ILK shRNA, T315 dose-dependently suppressed the expression level of Notch1^{NICD}, without affecting the full-length Notch1, in MDA-MB-231 and SUM-159 cells (Figure 2A). This finding was confirmed by the clearance of Notch1^{NICD} immunostaining from the nuclei of T315-treated MDA-MB-231 cells (Figure 2B), as well as the dose-dependent suppressive effect of T315 on Notch reporter activity (Figure 2C) and the expression of various Notch downstream targets (Figure 2D), including HES1 [24], c-Myc [25], Nestin [26], and ABCG2 [27], in both MDA-MB-231 and SUM-159 cells. It is noteworthy that T315-mediated down-regulation of these Notch targets was accompanied by parallel decreases in the expression of CSC-associated epithelial-mesenchymal transition regulators, including zinc finger E-box binding homeobox 1 (ZEB1) [28], Twist [29], and Y

box-binding protein 1 [30], which were also reported to be downstream effectors of ILK [13,31] (Figure 2D). Moreover, T315 was equipotent in downregulating other CSC-associated markers, including the Wnt signaling effector β-catenin and the hedgehog signaling effector Bmi1 (Figure 2D). Together, these findings suggest the ability of T315 to suppress the breast CSC subpopulation by targeting Notch1 and other CSC-associated pathways in IL-6–producing MDA-MB-231 and SUM-159 cells.

ILK Regulates the Assembly of Functional γ-Secretase Complex

Mechanistically, Notch activation requires γ-secretase–mediated cleavage of Notch to release Notch1^{NICD} into the nucleus to facilitate transcriptional regulation of target gene expression [32]. Thus, we hypothesize that the effect of ILK on Notch activation was associated with its ability to regulate γ-secretase–facilitated Notch1 cleavage. To examine this mechanistic link, ILK was overexpressed in MCF-7 cells to elicit Notch activation, which, as expected, increased the expression of Notch1^{NICD} and its targets, including HES1, c-Myc, Nestin, and ABCG2 (Figure 3A). Treatment with the γ-secretase inhibitor, DAPT, blocked this ILK-induced Notch activation, as evidenced by the reduced expression of the aforementioned Notch targets to basal levels (Figure 3A).
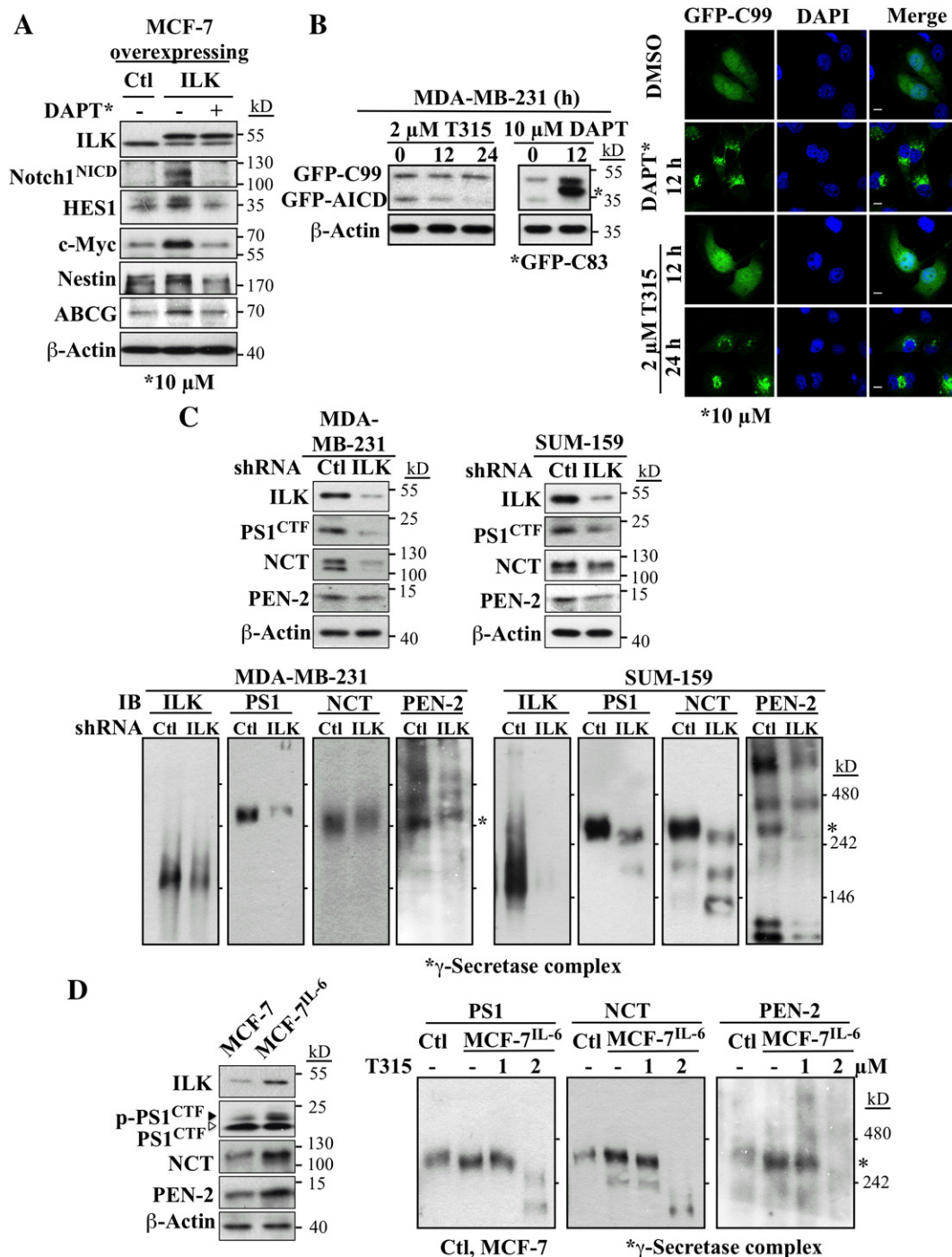
Figure 3. ILK is important for formation of functional γ-secretase complexes. (A) Immunoblot analysis of the effect of the γ-secretase inhibitor, DAPT (10 μM), on the expression of Notch1[NICD] and Notch downstream targets in MCF-7 cells that ectopically express ILK. Ctl, pCMV control. (B) Left: effects of T315 (2 μM) and DAPT (10 μM; 12- and/or 24-hour treatment) on the processing of GFP-C99 to GFP–amyloid precursor protein intracellular domain in MDA-MB-231 cells by immunoblot analysis. Right: Immunocytochemical analysis of the cellular distribution of the GFP fluorescence in GFP-C99-expressing MDA-MB-231 cells treated with T315 (2 μM) or DAPT (10 μM) (original magnification, ×60; scale bar, 10 μm). (C) Use of SDS-PAGE (upper) and Blue Native PAGE (lower), followed by immunoblot analysis, to analyze the suppressive effect of shRNA-mediated knockdown of ILK on native γ-secretase protein assemblies in the membranes of MDA-MB-231 and SUM-159 cells. (D) Use of SDS-PAGE (left) and Blue Native PAGE (right) to assess the dose-dependent effect of T315 on γ-secretase complex formation in MCF-7[IL-6] cells.

Pursuant to this finding, the ability of ILK to regulate γ-secretase enzyme activity was verified by the suppressive effect of T315 *vis-à-vis* DAPT on the processing of GFP-tagged C-terminal fragment of amyloid precursor protein (GFP-C99), a substrate for γ-secretase [33], to form the corresponding soluble intracellular domain (GFP–amyloid precursor protein intracellular domain; Figure 3B, *left panel*). However, in contrast to DAPT, T315 also blocked the formation of GFP-C83, which has been reported to be generated

from the endogenous α-secretase activity of GFP-C99 [34], and thus accumulated when γ-secretase activity was inhibited [33]. This finding suggests that T315 might also concomitantly block α-secretase activity. Moreover, confocal images of MDA-MB-231 cells transiently expressing GFP-C99 revealed that, under basal conditions, the GFP fluorescence is homogeneously distributed in the cytoplasm and nucleus, indicating γ-secretase–mediated cleavage of membrane-bound GFP-C99 (DMSO; Figure 3B, right panel). In contrast, exposure of these cells to T315 or DAPT blocked the γ-secretase–mediated cleavage, resulting in the majority of GFP fluorescence remaining as membrane-associated punctate structures. Moreover, we established a stable clone of MDA-MB-231 cells that overexpress ILK shRNA under Tet-on control (MDA-MB-231$^{TRE-ILK\ shRNA}$). The effect of doxycycline-induced knockdown of ILK on GFP-C99 cleavage paralleled that observed in T315-treated MDA-MB-231 cells (Supplementary Figure S2).

Active γ-secretase is a multiprotein complex composed of PS1, NCT, PEN-2, and anterior pharynx-defective protein 1. The full-length PS1 is endoproteolytically processed into two fragments, the N-terminal fragment and the C-terminal fragment [35], of which PS1^{CTF} is essential to γ-secretase activity [36]. Evidence indicates that these γ-secretase components require proper serial assembly steps or would undergo rapid degradation [36]. To shed light onto how ILK inhibition by T315 inhibited γ-secretase enzyme activity, we used Blue Native polyacrylamide gel electrophoresis (PAGE) to assess the effect of shRNA-mediated knockdown of ILK on γ-secretase protein assemblies in MDA-MB-231 and SUM-159 cells by following an established procedure [37]. Immunoblot analysis with antibodies specific for individual components of the complex, including PS1^{CTF}, NCT, and PEN-2 (Figure 3C, lower panel), indicated that silencing of ILK in either cell line resulted in the disappearance of the γ-secretase complex as a result of decreased expression of γ-secretase components (Figure 3C, upper panel). A similar disruption of the γ-secretase complex was also observed in T315-treated MCF-7^{IL-6} cells. In line with the reported effect of IL-6 on Notch activation [4,5], stable IL-6 overexpression in the MCF-7^{IL-6} cells increased expression of γ-secretase components (Figure 3D, left panel), leading to higher abundance of γ-secretase complexes than in the parental MCF-7 cells, as demonstrated by Blue Native PAGE (Figure 3D, right panel). Reminiscent of the results observed in ILK-silenced MDA-MB-231 and SUM-159 cells, T315 blocked this IL-6–induced increase in γ-secretase complex assembly in a dose-dependent manner. Considering the nature of γ-secretase activity on Notch cleavage, we also assessed the effect of T315 on the activation of different Notch isoforms in MDA-MB-231 cells (Supplementary Figure S3). Indeed, T315 suppressed the formation of the NICDs of Notch1, Notch2, and Notch3 but not Notch4, which is known to be more resistant to the γ-secretase inhibitor DAPT. [38] Together, the above findings suggest a putative role of ILK in mediating the effect of IL-6 on Notch1 activation through γ-secretase complex assembly.

ILK Regulates the Localization of the γ-Secretase Complex at Caveolae

It is noteworthy that ILK knockdown in MDA-MB-231 cells or stable IL-6 expression in MCF-7 cells did not alter the mRNA levels of the γ-secretase components PS1, NCT, and PEN-2 (Supplementary Figure S4), suggesting that the regulation was mediated at the posttranscriptional level. Indeed, the results described above showed

that ILK could support γ-secretase complex assembly by regulating expression of γ-secretase component proteins. We hypothesized that ILK could also regulate γ-secretase by affecting its localization to lipid rafts, of which the rationale is two-fold. First, it has been reported that the activation of γ-secretase is associated with its translocation to lipid rafts [39,40]. Second, ILK was reported to form complexes with caveolin-1 [18], which is essential to the formation of caveolae. This complex formation with ILK was reported to facilitate the correct positioning of caveolin-1 close to the cytoplasmic membrane [41]. Pursuant to this hypothesis, we examined the effect of ILK knockdown on the membrane localization of γ-secretase. In MDA-MB-231$^{TRE-shILK}$ cells, doxycycline-induced ILK knockdown facilitated gradual down-regulation, starting at 24 hours, of the expression of ILK and the γ-secretase components PS1, NCT, and PEN-2 (Figure 4A). Accordingly, we examined the effect of doxycycline-induced ILK knockdown on the cellular distribution of PS1, the catalytic core of γ-secretase, in MDA-MB-231$^{TRE-shILK}$ and MCF-7$^{IL-6/TRE-shILK}$ cells at 24 hours of doxycycline treatment. Immunocytochemical analysis indicated that, in the absence of doxycycline, the IL-6–producing MDA-MB-231$^{TRE-shILK}$ and MCF-7$^{IL-6/TRE-shILK}$ cells exhibited enriched association of PS1 with caveolae relative to the IL-6–deficient MCF-7 cells, as shown by the co-localization of PS1 staining with that of the caveolae/lipid raft markers GM1 ganglioside, which was detected by Alexa Fluor 647–conjugated cholera toxin B staining, and caveolin-1 (Figure 4, B and C). However, this association of PS1 with caveolae was blocked by doxycycline-induced ILK knockdown or T315, providing evidence in support of our hypothesis.

ILK Regulates the Assembly/Stability of the γ-Secretase Complex through Caveolin-1

Pursuant to these findings, we examined the effect of ILK knockdown on the association of PS1^{CTF} and NCT with lipid raft membrane fractions in MCF-7$^{IL-6/TRE-shILK}$ cells (Figure 5A). In line with the above immunocytochemical data, MCF-7$^{IL-6/TRE-shILK}$ cells, in the absence of doxycycline, showed substantially higher levels of caveolin-1, phospho-PS1^{CTF}, and NCT in the lipid raft fraction than MCF-7 cells, and knockdown of ILK was accompanied by parallel decreases in the lipid raft association of these three proteins. Consistent with the reported mobility shift of PS1^{CTF} after phosphorylation [42], phospho-PS1^{CTF} was enriched in lipid rafts, which is crucial to γ-secretase activity [43]. It is interesting to note that lipid raft–associated caveolin-1 exhibited a higher molecular mass than that of the non-lipid raft counterpart. As caveolin-1 is known to be palmitoylated in the course of transporting cholesterol to caveolae [44], this discrepancy might be attributable to this posttranslational modification of caveolin-1 in the lipid raft fraction. On the basis of this finding, we hypothesized that ILK might regulate the assembly of the γ-secretase complex in lipid raft microdomains by virtue of its reported regulatory role on caveolin-1. We obtained two lines of evidence in MCF-7$^{IL-6/TRE-shILK}$ cells to support this premise. First, co-immunoprecipitation experiments indicated the physical interaction of phospho-PS1^{CTF} and NCT with caveolin-1, which could be reduced by doxycycline-induced ILK knockdown (at 24 hours) or T315 treatment (Figure 5B). Second, knockdown of caveolin-1 with two different siRNAs decreased the localization of PS1^{CTF} and NCT to the lipid raft fraction (Figure 5C, right panel), which resulted in decreased γ-secretase activity, as manifested by reduced Notch1^{NICD} formation detected in cell lysates (Figure 5C, left panel). Together,
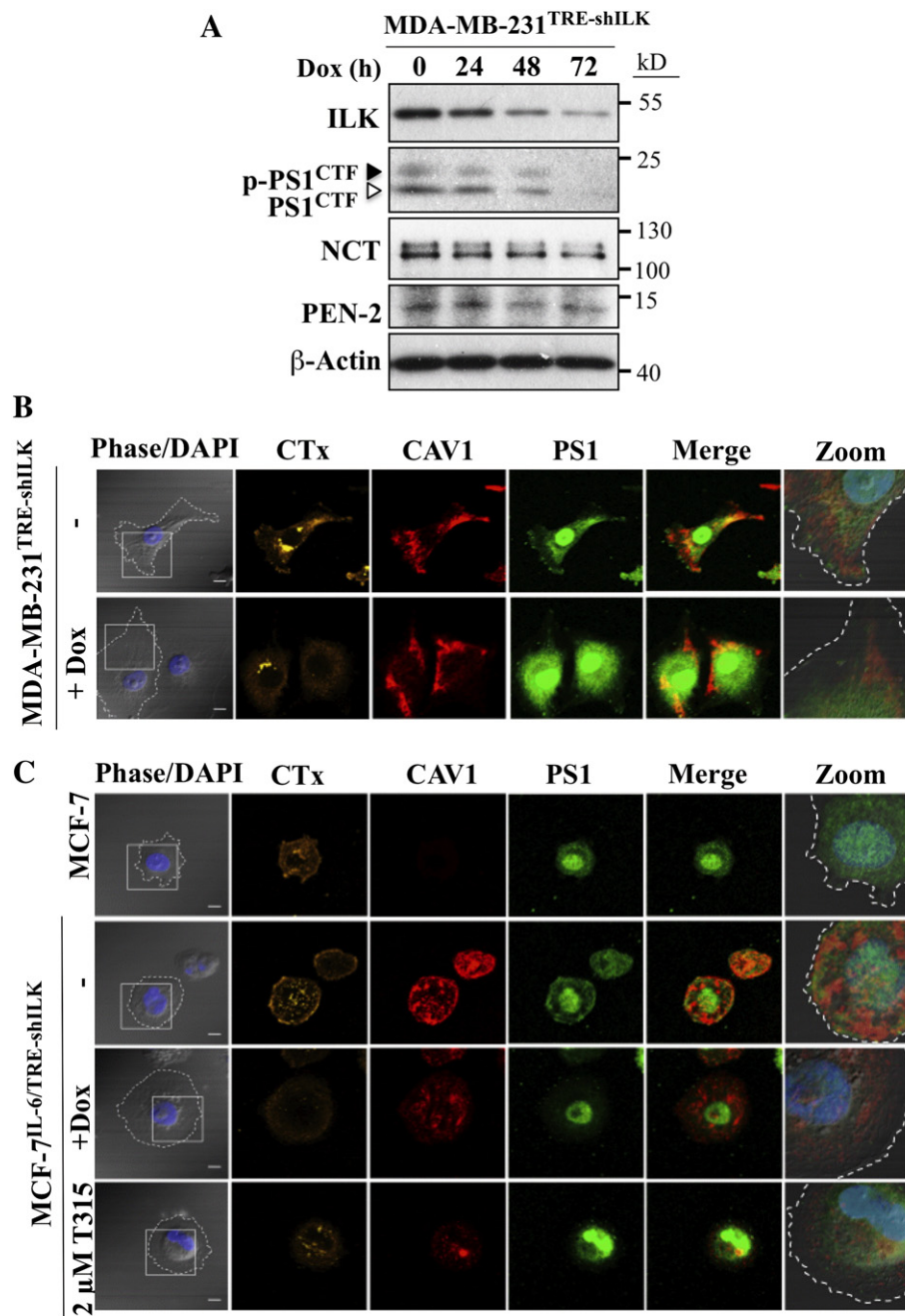
Figure 4. ILK regulates the localization of the γ-secretase complex at caveolae/lipid rafts. (A) Time-dependent effect of doxycycline (Dox)–inducible shRNA-mediated knockdown of ILK on the abundance of γ-secretase component proteins (PS1[CTF], NCT, and PEN-2) in MDA-MB-231[TRE-shILK] cells. (B and C) Immunocytochemical analyses of the effects of Dox-induced knockdown of ILK for 24 hours on the localization of PS1 to caveolae in (B) MDA-MB-231[TRE-shILK] cells and (C) MCF-7[IL-6/TRE-shILK] cells. The effects of T315 (2 μM) were also evaluated in MCF-7[IL-6/TRE-shILK] cells. Caveolae were identified by co-labeling with caveolin-1 antibody and Alexa Fluor 647–conjugated cholera toxin B (CTx) staining for lipid rafts. MCF-7 cells were used as a negative control. The rectangles in the phase/DAPI images indicate the areas magnified in the zoom images, in which the phase/DAPI images and the merged images were merged and magnified. The dotted lines indicate the edges of cell membranes. Scale bar, 10 μm.

these findings suggest that the effect of ILK on Notch1 activation was mediated through caveolin-1–dependent localization of the γ-secretase complex to caveolae/lipid rafts.

ILK Is Involved in Regulating Breast CSCs In Vivo

IL-6 has been reported to facilitate breast CSC expansion through the inflammatory feedback loop [45]. From a mechanistic perspective, the ability of ILK to stimulate Notch signaling through

γ-secretase activation might provide a molecular basis to account for the unique ability of IL-6 to facilitate the conversion of non–stem cancer cells to CSCs [45]. To verify this hypothesis, we assessed the effect of ILK inhibition on mammosphere formation in anchorage-independent, serum-free culture conditions, which represents a surrogate measure of CSC expansion [21,46]. Stable clones of ILK shRNA-expressing MDA-MB-231 and SUM-159 cells exhibited a diminished ability to form mammospheres relative to the respective
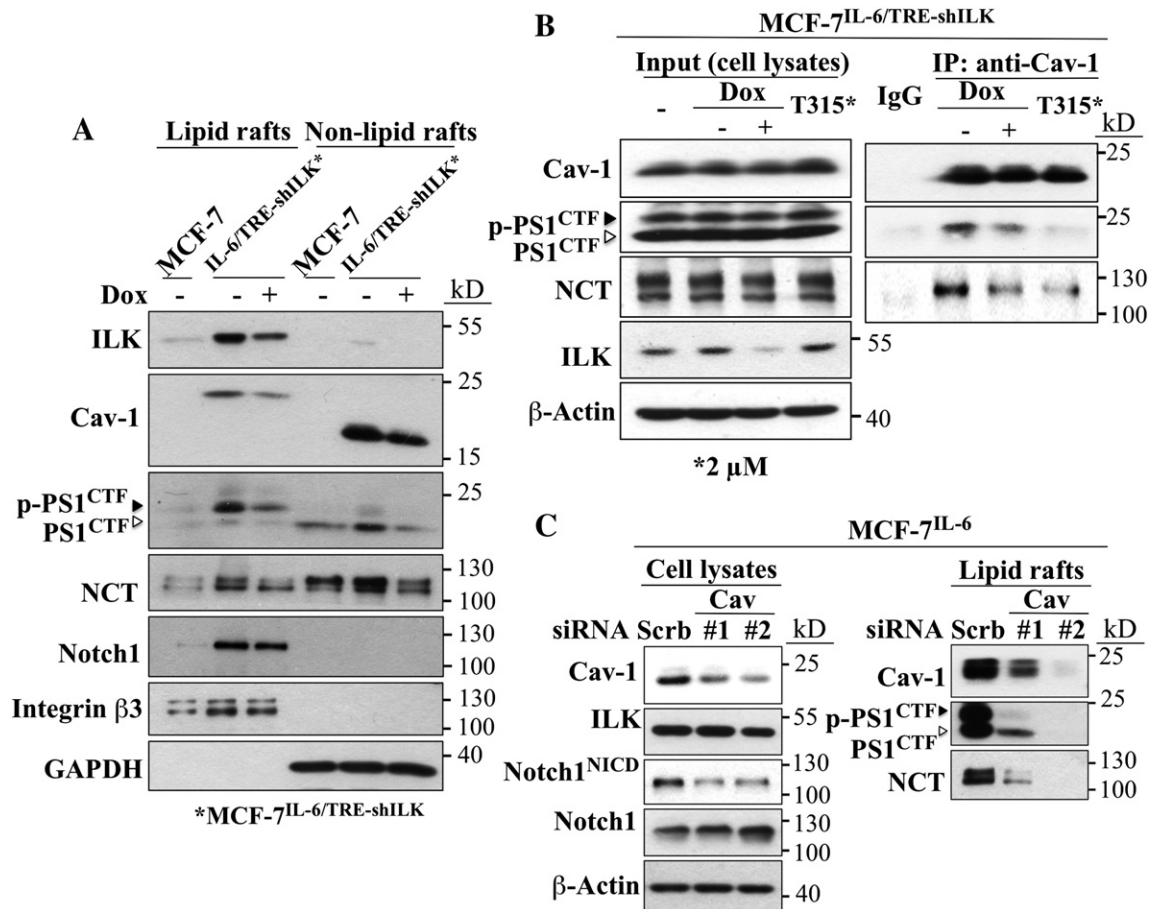
Figure 5. ILK regulates the assembly/stability of the γ-secretase complex at caveolae. (A) The distribution and relative expression of ILK, caveolin-1 (Cav-1), phospho-PS1CTF, PS1CTF, NCT, Notch1, integrin β3 (lipid raft–associated protein), and GAPDH (glyceraldehyde 3-phosphate dehydrogenase; non–lipid raft associated protein) in the lipid raft and non–lipid raft fractions in MCF-7 *versus* MCF-7[IL-6/TRE-shILK] cells with and without doxycycline (Dox) treatment (24 hours). (B) Co-immunoprecipitation analysis of complex formation of caveolin-1 with the γ-secretase components PS1CTF and NCT in MCF-7[IL-6/TRE-shILK] cells, and the suppressive effect of Dox-induced shRNA-mediated ILK knockdown and T315 (2 μM) for 24 hours on this complex formation. (C) Suppressive effects of siRNA-mediated knockdown of caveolin-1 (Cav) on Notch1 activation (left) and lipid raft localization of PS1CTF and NCT (right) in MCF-7[IL-6] cells.

controls (Figure 6A). Moreover, as CSCs are characterized by their capability to form tumors from low cell numbers, we assessed the effect of ILK knockdown on tumor initiating ability by injecting 50,000 stable ILK shRNA-expressing (MDA-MB-231[ILK KD]) or control (MDA-MB-231[Ctl KD]) MDA-MB-231 cells into the mammary fat pads of NOD/SCID mice. Although ILK-knocked-down cells were able to form tumors in all injected mice, they grew at a relative slower rate (Figure 6B).

Pursuant to the above findings, we used T315 as a proof-of-concept to demonstrate the therapeutic relevance of targeting ILK to suppress the breast CSC population *in vivo* by using a previously reported SUM-159 xenograft tumor model [20]. NOD/SCID mice bearing established SUM-159 tumors (50-70 mm³) in mammary fat pads were treated with T315 at 50 mg/kg twice daily by oral gavage or with vehicle. T315 reduced tumor volume by 70% by the end of the 11-day treatment (Figure 6C). The twice-daily oral administration of T315 was well tolerated, as no overt signs of toxicity and no loss of body weight were observed.

Reminiscent of the *in vitro* effects of T315 (Figure 2A), this suppression of tumor growth in T315-treated mice was associated with a 75% reduction in the abundance of intratumoral Notch1[NICD], relative to vehicle control ($P < .001$; Figure 6D). Moreover, the ability of

T315 to suppress the CSC subpopulation in these xenograft tumors was corroborated by two lines of evidence. First, ALDEFLUOR analysis of aldehyde dehydrogenase activity, a breast CSC marker [47], and mammosphere formation assays of dispersed tumor cells revealed that T315 treatment led to approximately 60% reduction in the ALDH[br] population and mammosphere formation (Figure 6E) relative to that in control mice. Second, we assessed the ability of dispersed tumor cells isolated from T315- and vehicle-treated SUM-159 tumor-bearing mice to initiate tumors on secondary reimplantation of 1000 cells in mammary fat pads of naive NOD/SCID mice. As shown in Table 1, only one of eight mice serially transplanted with re-isolated T315-treated SUM-159 tumor cells developed a palpable tumor, while five of eight in the control group formed tumors by 7 weeks post-injection, confirming the *in vivo* suppressive effect of T315 on the breast CSC population within tumors. Together, these findings suggest the translational potential of targeting ILK to suppress breast CSCs, which warrants further investigations.

Discussion

ILK has been reported to play a dichotomous role, either as an activator or as a suppressor, in regulating Notch in different biologic
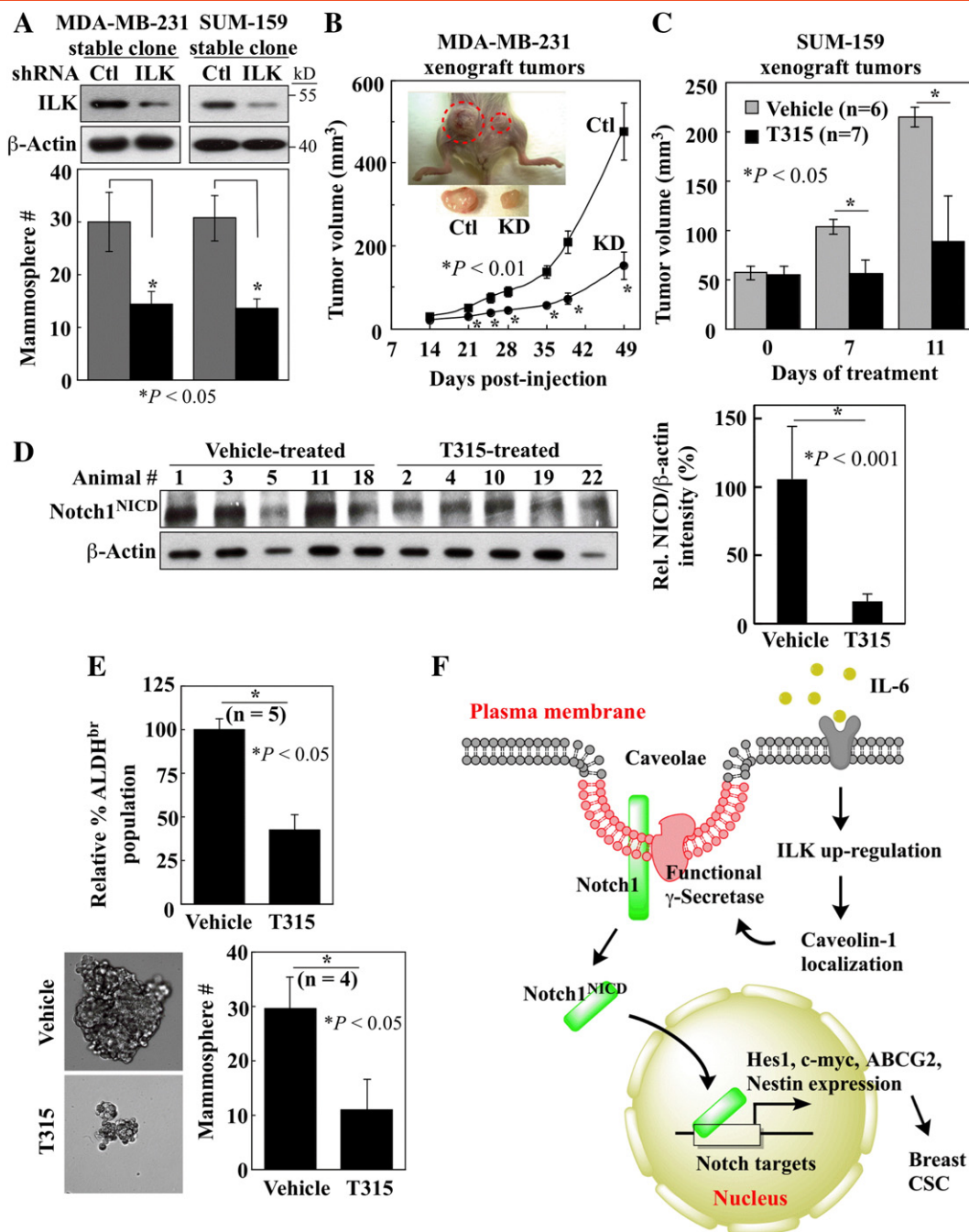
Figure 6. ILK is required for breast CSCs in *vivo*. (A) Suppressive effect of stable shRNA-mediated ILK knockdown on mammosphere formation by MDA-MB-231 and SUM-159 cells. Data are presented as means ± SD (n = 3). (B) Suppressive effect of stable shRNA-mediated ILK knockdown on MDA-MB-231 xenograft tumor growth in nude mice. Control and ILK knocked-down MDA-MB-231 cells (5×10^4 cells/mouse) were injected into the right and left inguinal mammary fat pads, respectively, of NOD/SCID mice, and tumor volumes were calculated from serial caliper measurements. (Inset) Images of control (Ctl) and ILK knocked-down (KD) xenograft tumors before and after dissection from a representative tumor-bearing mouse. Data are presented as means ± SEM (n = 6). (C) Suppressive effect of oral T315 (50 mg/kg, twice daily) on SUM-159 xenograft tumor growth in NOD/SCID mice after 7 and 11 days of treatment. (D) Western blot analysis of the effect of T315 on the abundance of Notch1[NICD] in SUM-159 xenograft tumors. Left: Immunoblot of five representative tumors from each group. Right: Corresponding densitometric analysis expressed as relative expression of Notch1[NICD], after normalization to β-actin (means ± SD; *P < .001 compared with vehicle). (E) Top: T315 decreased the percentage of the ALDH[br] subpopulation in SUM-159 xenograft tumors, as determined by ALDEFLOUR assays using tumor cells isolated from T315-treated *versus* vehicle-treated SUM-159 tumor-bearing mice. Data are presented as means ± SD (n = 5). Bottom: T315 diminished the mammosphere-forming ability of tumor cells isolated from T315-treated *versus* vehicle-treated SUM-159 tumor-bearing mice. Data are presented as means ± SD (n = 4). (F) Diagram depicting the role of ILK in regulating IL-6–induced Notch1 activation and CSC expansion through γ-secretase assembly at the caveolae.

Table 1. Tumorigenicity of SUM-159 Tumors Cells Harvested from T315- and Vehicle-Treated Mice and Reimplanted into Mammary Fat Pads of Naive Mice (1000 Cells per Mouse).

Treatment of Primary Tumor-Bearing Mice (*per os*, Twice Daily)	Tumor Incidence in Secondary Mice ($n = 8$) at 3 and 7 Weeks after Tumor Cell Reimplantation	
	3 Weeks	7 Weeks
Vehicle	3/8	5/8
T315	1/8	1/8

systems. For example, ILK was shown to activate Notch through Akt/GSK3β and Wnt signaling pathways in leukemic cells [14] and during somitogenesis in chicken embryo [15], respectively. Conversely, ILK was demonstrated to directly bind and phosphorylate Notch^{NICD}, thereby promoting Fbw7-facilitated proteasomal degradation of Notch^{NICD}, in NIH3T3 and HEK 293 cells [16]. This discrepancy underscores the complexity of the role of ILK in regulating Notch signaling in different malignant *versus* nonmalignant cell systems.

Within this context, we propose a new mechanism by which ILK facilitates IL-6–driven Notch1 activation by regulating the assembly/stability of the γ-secretase complex (Figure 6*F*). Specifically, ILK is responsible for the localization of γ-secretase to caveolae, leading to Notch1 cleavage to release Notch1^{NICD}. Accordingly, our data showed that the siRNA-mediated knockdown or pharmacological inhibition of ILK led to the disassembly/instability of γ-secretase, leading to reduced Notch^{NICD} release from Notch1 and other Notch isoforms. As ILK has been reported to be present in caveolae-enriched membranes and contains a putative caveolin-binding domain [18], we hypothesized that the effect of ILK on γ-secretase assembly/stability might be mediated through caveolin-1, although the exact mechanism remains unclear. This premise was supported by the formation of PS1^{CTF}–caveolin-1 complexes and the ability of ILK knockdown or T315 to reduce this physical interaction between PS1 and caveolin-1 and, consequently, γ-secretase activity. Although ILK mediates Ser473-Akt phosphorylation in response to IL-6 stimulation in breast cancer cells, our data suggest that this IL-6–driven Notch1 activation was independent of Akt signaling, as the PI3K inhibitor LY294002 exhibited no appreciable suppressive effect on Notch1^{NICD} expression in MCF-7^{IL-6} cells (Figure 1*F*). Moreover, our data indicate that ILK was not involved in IL-6–stimulated up-regulation of Notch1 expression in breast cancer cells, despite a recent report that Akt activated Notch1 gene expression through NF-κB in melanoma [22],

The mechanism by which ILK regulates the assembly/stability of the γ-secretase complex in caveolae is currently under investigation. It is plausible that ILK might phosphorylate γ-secretase components, thereby facilitating their interaction with caveolin-1. Alternatively, ILK might act as a scaffold protein to mediate the localization of γ-secretase to caveolae. It has been reported that ILK regulates caveolar trafficking by controlling microtubule dynamics and that loss of ILK function impairs the transport of caveolin-1–containing vesicles along microtubules to the plasma membrane to form new caveolae. The functional role of ILK in this regard is to recruit IQGAP1 and stabilize microtubules locally following insertion of caveolae into the plasma membrane [48]. Although T315 was developed as an ILK kinase inhibitor that competes with ATP binding, the ability of T315 to block this localization raises a

possibility that T315 binding might induce conformational changes that prohibit the interaction of ILK with its binding partner.

Although active γ-secretase is known to localize to lipid rafts, our findings suggest that the interaction between γ-secretase and caveolin-1 is essential for directing the localization of γ-secretase to caveolae, specialized membrane microdomains that can regulate multiple signaling pathways, including those mediated by c-Met, the type I insulin-like growth factor receptor, matrix metalloproteases, estrogen receptor, and IL-6. As clinical evidence has implicated upregulated caveolin-1 expression in the tumorigenesis of multiple epithelial tumors [49], how caveolin-1 regulates Notch1 activation warrants further investigations.

To date, more than 100 γ-secretase inhibitors have been developed to target Notch signaling, many of which are currently in clinical trials. The mechanism by which the ILK inhibitor T315 inhibits γ-secretase enzyme activity is distinct from that of known γ-secretase inhibitors [50] and thus might have therapeutic value in circumventing resistance of cancer cells to γ-secretase inhibitors. For example, it has been reported that loss of phosphatase and tensin homolog (PTEN) function in T-cell acute lymphoblastic leukemia led to resistance to γ-secretase inhibitors as a result of constitutive activation of Akt signaling [51]. In light of the frequent mutation or inactivation of PTEN in breast cancer [52], the targeting of ILK to suppress IL-6–driven Notch activation may be a rational therapeutic approach in patients with breast cancer.

In summary, we obtained *in vitro* and *in vivo* evidence that ILK plays an important role in mediating the IL-6–induced expansion of the breast CSC population through Notch activation (Figure 6*F*). Our data suggest that ILK regulates γ-secretase assembly/stability through a caveolin-1–dependent mechanism in caveolae. Therefore, targeting ILK might foster new therapeutic strategies to eliminate the CSC population in advanced metastatic breast cancer.

Appendix A. Supplementary data

Supplementary data to this article can be found online at http://dx.doi.org/10.1016/j.neo.2015.06.001.

References

[1] Vermeulen L, Todaro M, de Sousa Mello F, Sprick MR, Kemper K, Perez Alea M, Richel DJ, Stassi G, and Medema JP (2008). Single-cell cloning of colon cancer stem cells reveals a multi-lineage differentiation capacity. *Proc Natl Acad Sci U S A* **105**, 13427–13432.

[2] Visvader JE and Lindeman GJ (2008). Cancer stem cells in solid tumours: accumulating evidence and unresolved questions. *Nat Rev Cancer* **8**, 755–768.

[3] Liu S and Wicha MS (2010). Targeting breast cancer stem cells. *J Clin Oncol* **28**, 4006–4012.

[4] Sethi N, Dai X, Winter CG, and Kang Y (2011). Tumor-derived JAGGED1 promotes osteolytic bone metastasis of breast cancer by engaging notch signaling in bone cells. *Cancer Cell* **19**, 192–205.

[5] Sansone P, Storci G, Tavolari S, Guarnieri T, Giovannini C, Taffurelli M, Ceccarelli C, Santini D, Paterini P, and Marcu KB, et al (2007). IL-6 triggers malignant features in mammospheres from human ductal breast carcinoma and normal mammary gland. *J Clin Invest* **117**, 3988–4002.

[6] Klinakis A, Szabolcs M, Politi K, Kiaris H, Artavanis-Tsakonas S, and Efstratiadis A (2006). Myc is a Notch1 transcriptional target and a requisite for Notch1-induced mammary tumorigenesis in mice. *Proc Natl Acad Sci U S A* **103**, 9262–9267.

[7] Ling H, Sylvestre JR, and Jolicoeur P (2013). Cyclin D1-dependent induction of luminal inflammatory breast tumors by activated notch3. *Cancer Res* **73**, 5963–5973.

[8] Reedijk M, Odorcic S, Chang L, Zhang H, Miller N, McCready DR, Lockwood G, and Egan SE (2005). High-level coexpression of JAG1 and NOTCH1 is observed in human breast cancer and is associated with poor overall survival. *Cancer Res* **65**, 8530–8537.

[9] Speiser JJ, Ersahin C, and Osipo C (2013). The functional role of Notch signaling in triple-negative breast cancer. *Vitam Horm* **93**, 277–306.

[10] Al-Hussaini H, Subramanyam D, Reedijk M, and Sridhar SS (2011). Notch signaling pathway as a therapeutic target in breast cancer. *Mol Cancer Ther* **10**, 9–15.

[11] Legate KR, Montanez E, Kudlacek O, and Fassler R (2006). ILK, PINCH and parvin: the tIPP of integrin signalling. *Nat Rev Mol Cell Biol* **7**, 20–31.

[12] McDonald PC, Fielding AB, and Dedhar S (2008). Integrin-linked kinase—essential roles in physiology and cancer biology. *J Cell Sci* **121**, 3121–3132.

[13] Matsui Y, Assi K, Ogawa O, Raven PA, Dedhar S, Gleave ME, Salh B, and So AI (2012). The importance of integrin-linked kinase in the regulation of bladder cancer invasion. *Int J Cancer* **130**, 521–531.

[14] Tabe Y, Jin L, Tsutsumi-Ishii Y, Xu Y, McQueen T, Priebe W, Mills GB, Ohsaka A, Nagaoka I, and Andreeff M, et al (2007). Activation of integrin-linked kinase is a critical prosurvival pathway induced in leukemic cells by bone marrow–derived stromal cells. *Cancer Res* **67**, 684–694.

[15] Rallis C, Pinchin SM, and Ish-Horowicz D (2010). Cell-autonomous integrin control of Wnt and Notch signalling during somitogenesis. *Development* **137**, 3591–3601.

[16] Mo JS, Kim MY, Han SO, Kim IS, Ann EJ, Lee KS, Seo MS, Kim JY, Lee SC, and Park JW, et al (2007). Integrin-linked kinase controls Notch1 signaling by down-regulation of protein stability through Fbw7 ubiquitin ligase. *Mol Cell Biol* **27**, 5565–5574.

[17] Sasser AK, Sullivan NJ, Studebaker AW, Hendey LF, Axel AE, and Hall BM (2007). Interleukin-6 is a potent growth factor for ER-α-positive human breast cancer. *FASEB J* **21**, 3763–3770.

[18] Meyer A, van Golen CM, Boyanapalli M, Kim B, Soules ME, and Feldman EL (2005). Integrin-linked kinase complexes with caveolin-1 in human neuroblastoma cells. *Biochemistry* **44**, 932–938.

[19] Scherer PE, Tang Z, Chun M, Sargiacomo M, Lodish HF, and Lisanti MP (1995). Caveolin isoforms differ in their N-terminal protein sequence and subcellular distribution. Identification and epitope mapping of an isoform-specific monoclonal antibody probe. *J Biol Chem* **270**, 16395–16401.

[20] Li Y, Zhang T, Korkaya H, Liu S, Lee HF, Newman B, Yu Y, Clouthier SG, Schwartz SJ, and Wicha MS, et al (2010). Sulforaphane, a dietary component of broccoli/broccoli sprouts, inhibits breast cancer stem cells. *Clin Cancer Res* **16**, 2580–2590.

[21] Liao MJ, Zhang CC, Zhou B, Zimonjic DB, Mani SA, Kaba M, Gifford A, Reinhardt F, Popescu NC, and Guo W, et al (2007). Enrichment of a population of mammary gland cells that form mammospheres and have in vivo repopulating activity. *Cancer Res* **67**, 8131–8138.

[22] Bedogni B, Warneke JA, Nickoloff BJ, Giaccia AJ, and Powell MB (2008). Notch1 is an effector of Akt and hypoxia in melanoma development. *J Clin Invest* **118**, 3660–3670.

[23] Lee SL, Hsu EC, Chou CC, Chuang HC, Bai LY, Kulp SK, and Chen CS (2011). Identification and characterization of a novel integrin-linked kinase inhibitor. *J Med Chem* **54**, 6364–6374.

[24] Wurmbach E, Wech I, and Preiss A (1999). The *Enhancer of split* complex of *Drosophila melanogaster* harbors three classes of Notch responsive genes. *Mech Dev* **80**, 171–180.

[25] Palomero T, Lim WK, Odom DT, Sulis ML, Real PJ, Margolin A, Barnes KC, O'Neil J, Neuberg D, and Weng AP, et al (2006). NOTCH1 directly regulates c-MYC and activates a feed-forward-loop transcriptional network promoting leukemic cell growth. *Proc Natl Acad Sci U S A* **103**, 18261–18266.

[26] Shih AH and Holland EC (2006). Notch signaling enhances nestin expression in gliomas. *Neoplasia* **8**, 1072–1082.

[27] Bhattacharya S, Das A, Mallya K, and Ahmad I (2007). Maintenance of retinal stem cells by Abcg2 is regulated by notch signaling. *J Cell Sci* **120**, 2652–2662.

[28] Brabletz S, Bajdak K, Meidhof S, Burk U, Niedermann G, Firat E, Wellner U, Dimmler A, Faller G, and Schubert J, et al (2011). The ZEB1/miR-200 feedback loop controls Notch signalling in cancer cells. *EMBO J* **30**, 770–782.

[29] Hsu KW, Hsieh RH, Huang KH, Fen-Yau Li A, Chi CW, Wang TY, Tseng MJ, Wu KJ, and Yeh TS (2012). Activation of the Notch1/STAT3/Twist signaling axis promotes gastric cancer progression. *Carcinogenesis* **33**, 1459–1467.

[30] To K, Fotovati A, Reipas KM, Law JH, Hu K, Wang J, Astanehe A, Davies AH, Lee L, and Stratford AL, et al (2010). Y-box binding protein-1 induces the expression of *CD44* and *CD49f* leading to enhanced self-renewal, mammosphere growth, and drug resistance. *Cancer Res* **70**, 2840–2851.

[31] Kalra J, Sutherland BW, Stratford AL, Dragowska W, Gelmon KA, Dedhar S, Dunn SE, and Bally MB (2010). Suppression of Her2/neu expression through ILK inhibition is regulated by a pathway involving TWIST and YB-1. *Oncogene* **29**, 6343–6356.

[32] Sorensen EB and Conner SD (2010). γ-secretase-dependent cleavage initiates notch signaling from the plasma membrane. *Traffic* **11**, 1234–1245.

[33] Florean C, Zampese E, Zanese M, Brunello L, Ichas F, De Giorgi F, and Pizzo P (2008). High content analysis of gamma-secretase activity reveals variable dominance of presenilin mutations linked to familial Alzheimer's disease. *Biochim Biophys Acta* **1783**, 1551–1560.

[34] Kaether C, Schmitt S, Willem M, and Haass C (2006). Amyloid precursor protein and Notch intracellular domains are generated after transport of their precursors to the cell surface. *Traffic* **7**, 408–415.

[35] Thinakaran G, Borchelt DR, Lee MK, Slunt HH, Spitzer L, Kim G, Ratovitsky T, Davenport F, Nordstedt C, and Seeger M, et al (1996). Endoproteolysis of presenilin 1 and accumulation of processed derivatives in vivo. *Neuron* **17**, 181–190.

[36] Takasugi N, Tomita T, Hayashi I, Tsuruoka M, Niimura M, Takahashi Y, Thinakaran G, and Iwatsubo T (2003). The role of presenilin cofactors in the γ-secretase complex. *Nature* **422**, 438–441.

[37] LaVoie MJ, Fraering PC, Ostaszewski BL, Ye W, Kimberly WT, Wolfe MS, and Selkoe DJ (2003). Assembly of the γ-secretase complex involves early formation of an intermediate subcomplex of Aph-1 and nicastrin. *J Biol Chem* **278**, 37213–37222.

[38] Harrison H, Farnie G, Howell SJ, Rock RE, Stylianou S, Brennan KR, Bundred NJ, and Clarke RB (2010). Regulation of breast cancer stem cell activity by signaling through the Notch4 receptor. *Cancer Res* **70**, 709–718.

[39] Vetrivel KS, Cheng H, Lin W, Sakurai T, Li T, Nukina N, Wong PC, Xu H, and Thinakaran G (2004). Association of γ-secretase with lipid rafts in post-Golgi and endosome membranes. *J Biol Chem* **279**, 44945–44954.

[40] Wolfe MS (2013). Alzheimer's γ-secretase under arrestin. *Nat Med* **19**, 22–24.

[41] Malan D, Elischer A, Hesse M, Wickstrom SA, Fleischmann BK, and Bloch W (2013). Deletion of integrin linked kinase in endothelial cells results in defective RTK signaling caused by caveolin 1 mislocalization. *Development* **140**, 987–995.

[42] Seeger M, Nordstedt C, Petanceska S, Kovacs DM, Gouras GK, Hahne S, Fraser P, Levesque L, Czernik AJ, and George-Hyslop PS, et al (1997). Evidence for phosphorylation and oligomeric assembly of presenilin 1. *Proc Natl Acad Sci U S A* **94**, 5090–5094.

[43] Kuo LH, Hu MK, Hsu WM, Tung YT, Wang BJ, Tsai WW, Yen CT, and Liao YF (2008). Tumor necrosis factor-α–elicited stimulation of γ-secretase is mediated by c-Jun N-terminal kinase-dependent phosphorylation of presenilin and nicastrin. *Mol Biol Cell* **19**, 4201–4212.

[44] Uittenbogaard A and Smart EJ (2000). Palmitoylation of caveolin-1 is required for cholesterol binding, chaperone complex formation, and rapid transport of cholesterol to caveolae. *J Biol Chem* **275**, 25595–25599.

[45] Iliopoulos D, Hirsch HA, Wang G, and Struhl K (2011). Inducible formation of breast cancer stem cells and their dynamic equilibrium with non-stem cancer cells via IL6 secretion. *Proc Natl Acad Sci U S A* **108**, 1397–1402.

[46] Grimshaw MJ, Cooper L, Papazisis K, Coleman JA, Bohnenkamp HR, Chiapero-Stanke L, Taylor-Papadimitriou J, and Burchell JM (2008). Mammosphere culture of metastatic breast cancer cells enriches for tumorigenic breast cancer cells. *Breast Cancer Res* **10**, R52.

[47] Ginestier C, Hur MH, Charafe-Jauffret E, Monville F, Dutcher J, Brown M, Jacquemier J, Viens P, Kleer CG, and Liu S, et al (2007). ALDH1 is a marker of normal and malignant human mammary stem cells and a predictor of poor clinical outcome. *Cell Stem Cell* **1**, 555–567.

[48] Wickstrom SA, Lange A, Hess MW, Polleux J, Spatz JP, Kruger M, Pfaller K, Lambacher A, Bloch W, and Mann M, et al (2010). Integrin-linked kinase controls microtubule dynamics required for plasma membrane targeting of caveolae. *Dev Cell* **19**, 574–588.

[49] Burgermeister E, Liscovitch M, Rocken C, Schmid RM, and Ebert MP (2008). Caveats of caveolin-1 in cancer progression. *Cancer Lett* **268**, 187–201.

[50] Olsauskas-Kuprys R, Zlobin A, and Osipo C (2013). Gamma secretase inhibitors of Notch signaling. *Oncol Targets Ther* **6**, 943–955.

[51] Palomero T, Sulis ML, Cortina M, Real PJ, Barnes K, Ciofani M, Caparros E, Buteau J, Brown K, and Perkins SL, et al (2007). Mutational loss of PTEN induces resistance to NOTCH1 inhibition in T-cell leukemia. *Nat Med* **13**, 1203–1210.

[52] DeGraffenried LA, Fulcher L, Friedrichs WE, Grunwald V, Ray RB, and Hidalgo M (2004). Reduced PTEN expression in breast cancer cells confers susceptibility to inhibitors of the PI3 kinase/Akt pathway. *Ann Oncol* **15**, 1510–1516.